

A reactive phase diagram of CO oxidation on Pd(110): Steady and oscillatory states

Cite as: J. Chem. Phys. **98**, 9177 (1993); <https://doi.org/10.1063/1.464425>

Submitted: 06 July 1992 • Accepted: 15 February 1993 • Published Online: 31 August 1998

M. Ehsasi, M. Berdau, T. Reibitzki, et al.



View Online



Export Citation

ARTICLES YOU MAY BE INTERESTED IN

[Oscillatory CO oxidation on Pt\(110\): Modeling of temporal self-organization](#)

The Journal of Chemical Physics **96**, 9161 (1992); <https://doi.org/10.1063/1.462226>

[Macroscopic and mesoscopic characterization of a bistable reaction system: CO oxidation on Pt\(111\) surface](#)

The Journal of Chemical Physics **110**, 11551 (1999); <https://doi.org/10.1063/1.479097>

[Mathematical modeling of kinetic oscillations in the catalytic CO oxidation on Pd\(110\): The subsurface oxygen model](#)

The Journal of Chemical Physics **93**, 811 (1990); <https://doi.org/10.1063/1.459451>

Lock-in Amplifiers
up to 600 MHz



Zurich
Instruments



A reactive phase diagram of CO oxidation on Pd(110): Steady and oscillatory states

M. Ehsasi, M. Berdau, T. Rebitzki, K.-P. Charlé, K. Christmann,^{a)} and J. H. Block
Fritz-Haber-Institut der MPG, Faradayweg 4-6, D-14195 Berlin-Dahlem, Germany

(Received 6 July 1992; accepted 15 February 1993)

The steady and oscillatory regions of the CO oxidation reaction on the Pd(110) surface have been determined as a function of externally controlled parameters (flow rate, CO and oxygen partial pressures, temperature) over a wide range. At constant sample temperature and flow rate, the experiments yield a characteristic cross-shaped phase diagram separating regions of monostability, bistability, and oscillatory behavior. The existence of a cross-shaped phase diagram indicates the operation of a slow feedback process, which could be traced back to the (experimentally verified) formation and retarded removal of subsurface oxygen during the reaction. The diagram reflects one of the first well-defined oscillatory systems in heterogeneous catalysis and may provide a general basis for mechanistic studies and models of oscillatory surface reactions.

I. INTRODUCTION

Among the various chemical systems which exhibit oscillatory behavior for conditions far from equilibrium, the heterogeneous oxidation of CO on Pt group metals represents a frequently investigated model system.¹⁻¹³ Similar to many homogeneous reactions such as the well-known Belousov-Zhabotinskii (BZ) reaction,¹⁴⁻¹⁷ the CO oxidation over Pt metals also provides a rich variety of temporal oscillations and dissipative structures as recent experiments using photoelectron emission microscopy (PEEM) revealed.¹¹⁻¹³ Although the total number of reaction steps is considerably smaller in comparison with the BZ reaction, overall agreement between the observed features and the theoretical models has not been as good. The reason for this incongruity can be traced mainly to the experimental difficulties in obtaining a high degree of reproducibility in the measurement of oscillation parameters such as amplitude and frequency. Furthermore, the range of external control parameters under which the reaction shows bifurcations, e.g., transitions from steady state to oscillatory behavior, is either extremely narrow or hard to determine experimentally and does not provide the fine features which are crucial for comparisons with simulations and theoretical studies in general.¹⁷

The information about a system's steady-state or oscillatory behavior can be compiled in a kind of kinetic phase diagram. This term has been proposed—in analogy to equilibrium thermodynamics—by Schlögl in the 1970's,^{18,19} based on the fact that in both equilibrium and nonequilibrium phase transitions cooperative phenomena play a decisive role leading, for example, to ordered structures in the equilibrium and to self-organizing dissipative structures in the nonequilibrium case (which we deal with here). The occurrence of competing reactive "phases" is intimately correlated with instabilities, multistability, bifurcations, or kinetic oscillations. In the following, we shall, therefore,

denote any plot relating the system's reactivity behavior with state variables (p, T, \dots) as a "(reactive) phase diagram." For reactions in homogeneous phase, experimental phase diagrams showing different steady-state and oscillatory regimes have laid a basis for deriving mechanisms for oscillations or finding new oscillatory systems.²⁰

Among the single-crystal surfaces used for studying the heterogeneous CO oxidation the Pd(110) surface has thus far revealed the highest degree of reproducibility in its reactivity.^{9,10} As opposed to platinum surfaces (which frequently undergo reconstruction and/or faceting during the reaction and, hence, exhibit changes in the surface reactivity) the oscillatory behavior of CO oxidation on Pd(110) even at higher reactant pressures remains practically unchanged over long periods of experimenting. A common phenomenon observed with all Pt surfaces so far consists of very narrow oscillatory regions located close to the transition from low to high reactivity and vice versa. In our study we have, therefore, characterized the steady as well as the nonsteady reaction regions over a large range of the externally controlled parameters and have thus determined the first well-defined cross-shaped phase diagram for an oscillating system in heterogeneous catalysis.

II. EXPERIMENT

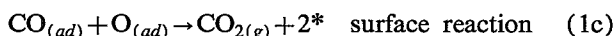
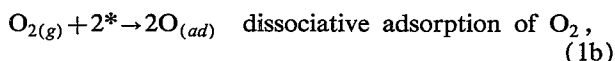
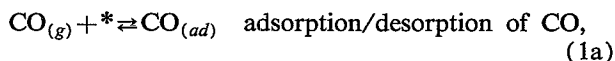
The experiments were performed in an ultra-high vacuum (UHV) cell (total volume ≈ 0.7 l) used as a flow reactor. The catalyst was a disk-shaped palladium (110) single crystal (effective area 32 mm^2 , thickness 1.5 mm). Cleaning was accomplished by a combination of argon ion sputtering, heating in oxygen (1000 K, $p_{\text{O}_2} \approx 5 \times 10^{-7}$ Torr) and annealing at 1200 K. Additionally purified high-grade purity gases (CO: 99.997%; O₂: 99.999%) were admitted to the reactor cell via all-metal leak valves; the pressure of both reactants was measured by means of a spinning rotor gauge as well as by an ion gauge and regulated to within 0.1% of their set values. The sample temperature was measured by a Chromel-Alumel thermocouple spot-welded to the rear of the crystal; an electronic

^{a)}Present address: Freie Universität Berlin, Institut für Physikalische und Theoretische Chemie, Takustr. 3, D-1000 Berlin 33, Germany.

regulator helped to keep T sufficiently constant (to within 0.1% of the set value). The reaction rate R_{CO_2} , i.e., the rate of CO_2 formation, could be simultaneously followed by a differentially pumped quadrupole mass spectrometer and by means of continuous work function change ($\Delta\Phi$) measurements using a Kelvin probe with a 10 mm^2 gold ring reference electrode as reported previously.^{9,10} We recall that on Pd(110) CO adsorption at 300 K increases the work function by 1050 mV at saturation, whereas oxygen saturation leads to a $\Delta\Phi$ of merely 700 mV under same conditions. It turned out from previous measurements^{9,10} and could again be confirmed in the present study that $\Delta\Phi$ basically monitors the CO surface concentration (coverage θ) and follows the CO_2 evolution (reaction rate R_{CO_2}) in every detail. Since $\Delta\Phi$ can be conveniently measured with high accuracy we have mainly used this quantity to monitor the reaction rate.

III. RESULTS

The oxidation of CO on Pt group metals follows the Langmuir–Hinshelwood (L–H) mechanism¹ where both CO and oxygen react from the adsorbed state. The decisive reaction steps are as follows:



(* denotes an empty surface site).

Not only does the rate of the catalytic CO oxidation on Pd surfaces depend on the abundance of the reactants in the gas phase (control parameters: p_{CO} , p_{O_2}) and the pumping speed F , but also on the details of possible surface processes such as adsorption, desorption, surface diffusion, and reaction of CO and oxygen, which, in turn, may crucially depend on temperature T (via activation energies). In order to sort out the influence of these variables we have, in our experiments, systematically varied these external control parameters F , p_i , and T and followed their effect on the reaction rate R_{CO_2} . By keeping three of the parameters constant and varying the fourth, one can clearly distinguish three regions with different behavior of the reactivity R_{CO_2} , namely: a high reactivity region, a low reactivity region and, in between, a region where, depending on the O_2 partial pressure, the reactivity exhibits either bistability or a more or less complex oscillatory behavior.

For the sake of clarity only the variation of the CO partial pressure with F , p_{O_2} , and T kept constant will be considered in the following. Then the three regions are determined by the corresponding ranges of p_{CO} as follows: Starting at low p_{CO} there is one and only one stable steady state with high reactivity, which loses stability at $p_{\text{CO}} = \tau_A(F, p_{\text{O}_2}, T)$. Likewise, at high CO pressures only a steady state with low reactivity exists, which becomes unstable at $p_{\text{CO}} = \tau_B(F, p_{\text{O}_2}, T)$. If $\tau_B < \tau_A$, then the high

reactivity state is globally stable for $p_{\text{CO}} \leq \tau_B$ and the low reactivity state is globally stable for $p_{\text{CO}} \geq \tau_A$. In the third intermediate region $\tau_B < p_{\text{CO}} < \tau_A$ the system is found, at least in the present system, in either of the two steady states, depending on the scan direction. This situation, where only steady states are involved, will be termed bistable (multistable) in the following. Likewise, $p_{\text{CO}} \leq \tau_B$ and $p_{\text{CO}} \geq \tau_A$ will be referred to as “regions of monostability” A and B . As compared to “global stability,” the more specific term “monostability” is introduced here in order to exclude both bistability and stationary oscillations, since the latter can be due to a globally stable limit cycle. In the case $\tau_A < \tau_B$ one has $p_{\text{CO}} \leq \tau_A$: region of monostability A and $p_{\text{CO}} \geq \tau_B$: region of monostability B . In the intermediate region $\tau_A < p_{\text{CO}} < \tau_B$ one finds either bistability or more frequently oscillations. The term “oscillations” or “oscillatory” will be used whenever at least one oscillatory state is involved. They are thus a rather raw characterization of the behavior of the system in the intermediate region. In summary, by scanning p_{CO} at constant F , p_{O_2} , and T one determines the CO partial pressures τ_A and τ_B , where the states of high reactivity and low reactivity become unstable. τ_A and τ_B are the boundaries between the regions of monostability and regions of either bistability or oscillatory behavior in control parameter space.

Two examples for lower and higher oxygen pressure p_{O_2} will clarify the procedure just described. In the first case (Fig. 1), one starts in the high-reactivity region A (also termed “oxygen side”), where the CO_2 production increases linearly with increasing p_{CO} until it reaches a maximum. Then it drops in a more or less narrow pressure range around τ_A to the low reactivity region B (also termed “CO side”); i.e., there is clearly a transition from high to low reactivity at τ_A . In this way we obtain a triangle-shaped reactivity curve which closely resembles the one found with a Pt(210) surface (cf. Fig. 6 of Ref. 7). If one now reduces p_{CO} gently back to the low starting value to complete a single cycle, the reactivity remains low and the transition into region A occurs at $\tau_B < \tau_A$. Thus the system is bistable in the intermediate region and exhibits consequently a pronounced (clockwise) hysteresis as is evident from Fig. 1. Note that for hystereses with a finite width there always exist two principally different possibilities, namely a hysteresis in the clockwise or the counter-clockwise sense. The orientation of the hysteresis of the CO_2 reaction rate is characterized by the location of the upward and downward transitions on the p_{CO} axis. A clockwise hysteresis is found for $\tau_A > \tau_B$, while for a counter-clockwise hysteresis $\tau_B > \tau_A$.

It is well known that a clockwise hysteresis, which is typical for low oxygen pressures, can be explained in principle by the reaction scheme (1) alone. The steady-state solution of the corresponding differential equations yields a (distorted) z-shaped dependence of the reactivity on p_{CO} for suitable values of the rate constants.^{21,22} One obtains two stable steady branches with larger oxygen coverages and larger CO coverages, respectively, and one unstable branch in between. The stable high reactivity branch, which emerges from region A , becomes marginally unsta-

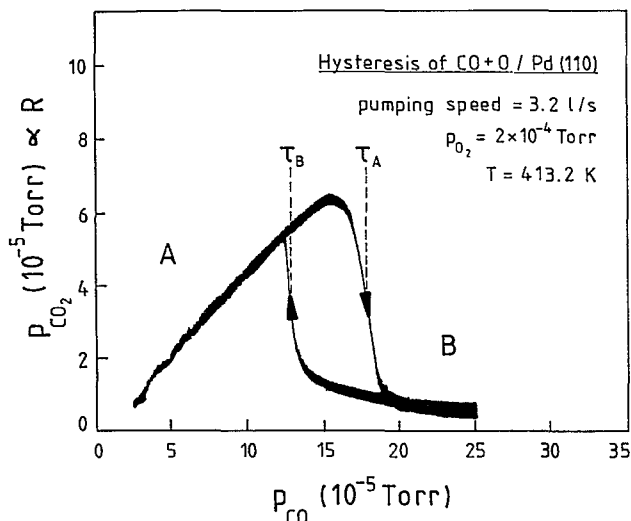


FIG. 1. The rate of CO_2 formation for increasing and decreasing CO partial pressure. τ_A and τ_B indicate the transition points from the oxygen-covered and CO-covered regions, respectively. The pressure ranges *A* and *B* represent the regions of monostable high and low reactivity states.

ble around τ_A and so does the low reactivity branch at τ_B . In other words, the instabilities at these points are saddle-node bifurcations. Because of the *z* shape of the reactivity curve one has $\tau_A > \tau_B$ and thus a clockwise hysteresis.

An example for higher oxygen pressure is shown in Fig. 2, where the CO partial pressure was slowly decreased. Departing from a monostable situation on the CO side ($p_{\text{CO}} > 1.5 \times 10^{-5}$ Torr) regular oscillations with finite amplitude are induced at $\tau_B \approx 1.45 \times 10^{-5}$ Torr. At $p_{\text{CO}} \approx 1.4 \times 10^{-5}$ Torr a mixed-mode behavior sets in, i.e., the

system switches between the just described CO-side oscillations and another type of oscillations, called oxygen-side oscillations in the following, which are observed for $p_{\text{CO}} \leq 1.2 \times 10^{-5}$ Torr. The characteristic feature of these oxygen-side oscillations is the decrease of their amplitude with decreasing p_{CO} . Thus they die out smoothly around $\tau_A \approx 0.7 \times 10^{-5}$ Torr, where the monostable region *A* is reached. Note that $\tau_B > \tau_A$, which is typical for higher oxygen pressures in this system. As a further complication, it is noticed that the oscillatory behavior of the oxygen-side oscillations is not uniform in general: one frequently observes period-doubling and other aperiodic behavior. By the way, we have taken the opportunity to once more illustrate by means of Fig. 2 the aforementioned one-to-one correspondence of the CO_2 partial pressure (a measure of the catalytic reactivity) and the accompanying work function change $\Delta\Phi$; one easily recognizes the agreement in intensity and phase even in this complicated example.

It should be clear by now that the complex behavior which can be observed at higher oxygen pressures in the intermediate region $\tau_A < p_{\text{CO}} < \tau_B$ is challenging, if not prohibitive. This is the more so, as the oscillatory behavior on the CO side, i.e., for p_{CO} in the vicinity of τ_B is very sensitive to external parameters and, so we feel, also to specimen preparation. A more detailed investigation of the oscillatory region aiming at a correspondingly more detailed phase diagram requires a substantially higher level of experimental system control than hitherto achieved. What is clearly established at the moment is the nature of the transitions at the boundaries τ_A and τ_B of the oscillatory region: at τ_B one finds always an abrupt or hard mode transition from the low reactivity state *B*, and at τ_A one observes always a soft mode transition between the steady

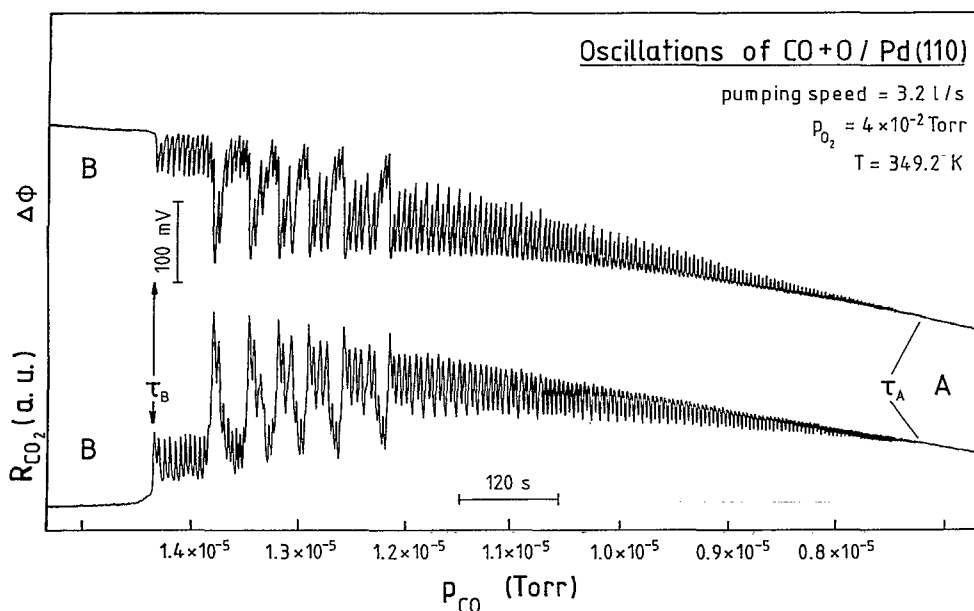


FIG. 2. The start of rate oscillations from the CO-covered side (region *B*) and the extent of the oscillatory region, for slowly decreasing CO pressure, as monitored by the work function change $\Delta\Phi$ (upper curve) and by the CO_2 partial pressure (lower curve). The transition points τ_A, τ_B and the external parameters are indicated in the figure.

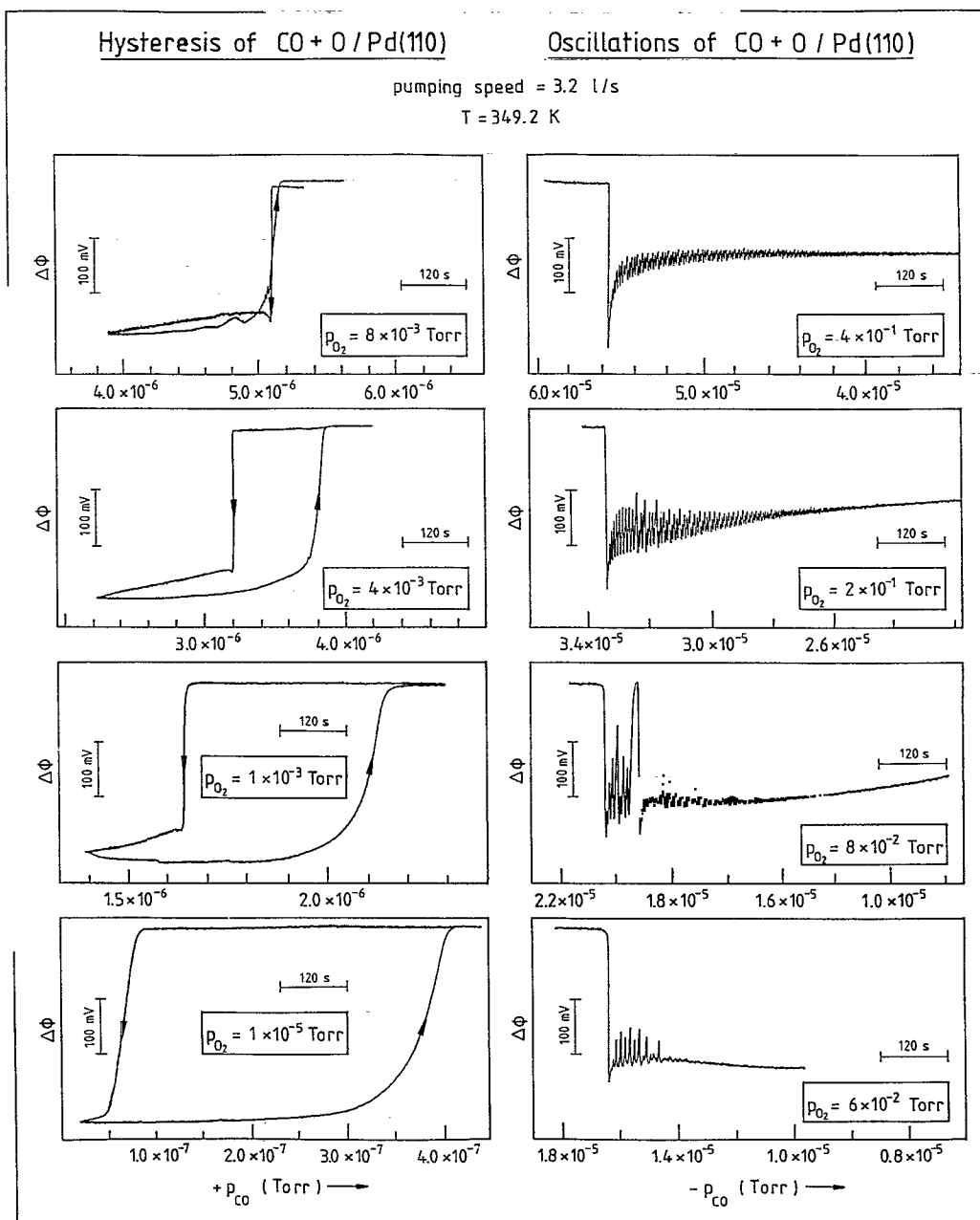


FIG. 3. (left column) Isothermal hysteresis in the work function change $\Delta\Phi$, for different oxygen partial pressures. (right column) p_{CO} scans through the oscillatory region for different oxygen partial pressures. The CO pressure was slowly decreased. The external parameters are indicated in the figure. See text for further details.

state A and the oxygen-side oscillations. The latter transition is readily recognized as a supercritical or normal Hopf bifurcation, whereas the experimental evidence for a subcritical Hopf bifurcation at τ_B is not so clear because of the just described difficulties on the CO side (see also Fig. 3, right column).

Experiments of the type shown in Figs. 1 and 2 were performed for various oxygen pressures extending from $\approx 10^{-5}$ to 4×10^{-1} Torr with the sample temperature being held constant at $T = 349.2$ K and the p_{CO} range being adjusted accordingly. The left-hand column of Fig. 3 dem-

onstrates that for all oxygen pressures below $\approx 10^{-2}$ Torr the surface only exhibits a clockwise hysteresis for the reactivity R_{CO_2} (counter-clockwise for $\Delta\Phi$!). However, as p_{O_2} approaches a value of $\approx 10^{-2}$ Torr, the hysteresis narrows more and more until the transition lines cross, at which time the direction of the hysteresis changes to a counter-clockwise rotation. Necessarily, one obtains a crossing point with $\tau_A = \tau_B$ which also signifies the onset of oscillations in the intermediate region. The appearance of oscillations for higher oxygen pressures is demonstrated in

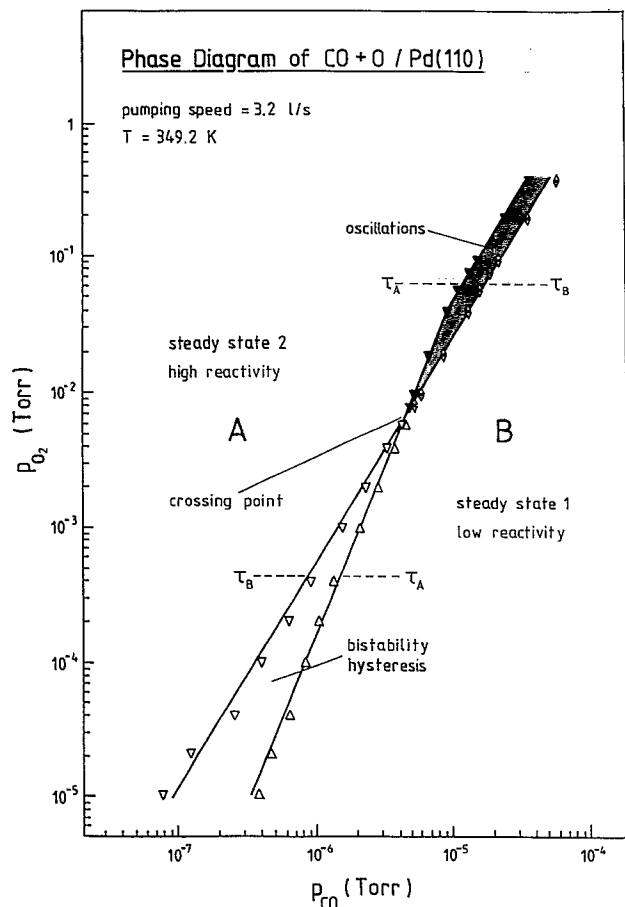


FIG. 4. The isothermal cross-shaped phase diagram with the various reactive regions. The external parameters are indicated in the figure.

the right-hand column of Fig. 3. The essential results of these experiments can be condensed in a phase diagram which is reproduced in Fig. 4. We have plotted therein those CO partial pressure values τ_A, τ_B where transitions occur during the p_{CO} scans, against the corresponding stationary oxygen pressure. The advantage of this kind of graphical representation is that the various reactive states of the surface can be clearly surveyed as a function of the gas phase concentration of the reactants. We have marked in Fig. 4 the monostable, bistable, and oscillatory regions; the lines τ_A and τ_B define the limit of the bistability region according to the remarks of Fig. 1. Beyond the crossing point, which we determine to lie, for the conditions chosen and indicated in Fig. 4, around $p_{CO} \approx 4 \times 10^{-6}$ Torr and $p_{O_2} \approx 7 \times 10^{-3}$ Torr, they constitute the boundaries of the oscillatory regions.

Whenever one deals with hysteresis phenomena it is legitimate to address the question as to how the observed features are time dependent, that is to say, how the width of the hysteresis depends on the scan speed of the control parameter (p_{CO} in our case). We have scrutinized this problem and note that the position of the transition lines, i.e., the limits of the bistable region) is only slightly affected by different ramping speeds, whereby an effect is especially noticeable at very low pumping speeds F . It was

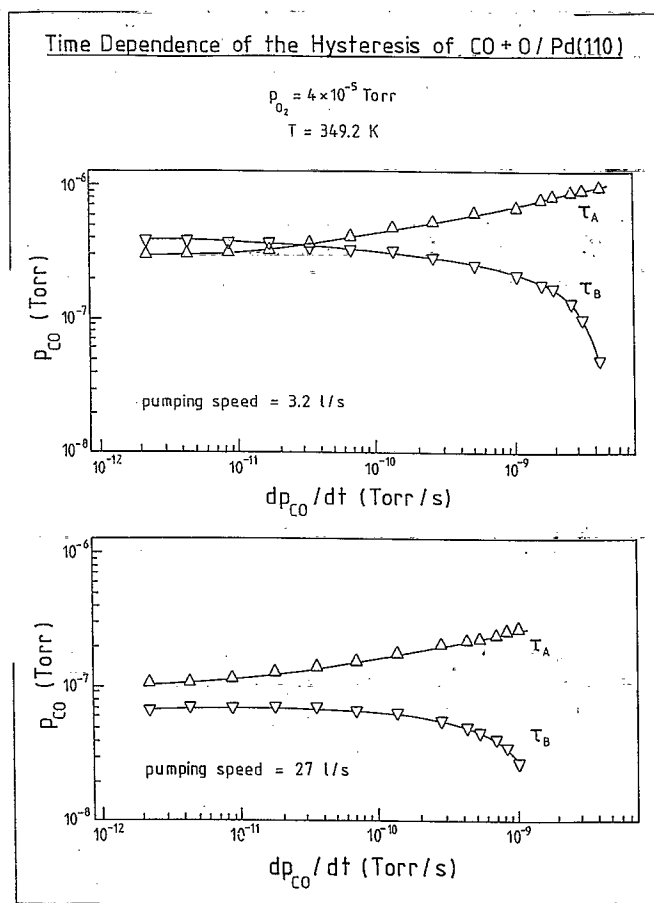


FIG. 5. The dependence of the transition points τ_A, τ_B on the p_{CO} scan speed for different pumping speeds as determined by $\Delta\Phi$ measurement. For $\tau_A > \tau_B$ the width of the clockwise hysteresis is $\tau_A - \tau_B$. Top curve: pumping speed $F = 3.2$ l/s; bottom curve: $F = 27$ l/s. The external parameters are indicated in the figure.

observed that for smaller scan speeds dp_{CO}/dt the crossing point moves toward somewhat lower oxygen pressures than those used to construct Fig. 4, however, without altering the overall principal shape of this cross-shaped phase diagram. Experiments carried out at lower pressures and higher pumping speeds, the results of which are compiled in Fig. 5, reveal that the transition points approach two different stable p_{CO} limits and that, for lower oxygen pressures, the system only exhibits hysteresis, but no longer oscillations. In other words, the hysteresis observed for lower oxygen pressures is genuine. For the lowest pumping speed ($F \approx 3.2$ l/s) the longest cycle time for increasing and decreasing the CO pressure was 128 h; it is superfluous to emphasize the extreme demands on cleanliness of such an experiment!

The main message of the experimental phase diagram (Fig. 4) is that the hysteresis behavior depicted schematically in Fig. 1 changes as we vary the experimental parameters. This is always evidence of the operation of an additional feedback process. If one models the catalytic CO oxidation merely on the basis of the L-H reaction steps (1) a bifurcation analysis of the steady-state equations clearly shows that the hysteresis remains unchanged for increasing oxygen partial pressure, that is to say, a crossing of the

hysteresis lines never occurs. The phase boundaries $\tau_A > \tau_B$ remain (in a logarithmic plot) parallel, and one can, from a corresponding phase diagram-plot, derive the approximate relation:

$$p_{\text{CO}} \propto \sqrt{p_{\text{O}_2}}$$

Our measurements show that with increasing oxygen pressure the influence of the responsible feedback process becomes stronger. Thus mostly the transition at τ_A from the oxygen side seems to be affected, although it is, admittedly, hard to determine which line is most influenced simply on the basis of a comparison of slopes (i.e., the slope of which transition line deviates most from the nominal value of 1/2).

Although we may anticipate part of the subsequent discussion section it may be useful to give a hint as to the possible nature of the aforementioned feedback process. We recall that a reversal in the direction of a hysteresis within the oscillatory region for CO oxidation on Pd(110) was also reported by Ladas *et al.*²³ The authors attributed this to a slow filling of oxygen atoms into the Pd subsurface regions. The appearance of an oxygen subsurface phase can, in turn, cause a reduction in the reactivity of the surface simply by reducing the sticking probability of oxygen and/or carbon monoxide.²⁴ A recovery or an increase in the reactivity, on the other hand, can take place when the subsurface oxygen is removed by diffusing back to the surface and reacting with adsorbed CO—a process that is likely to occur in a region where the surface is preferentially covered with CO (CO side). The formation of subsurface oxygen on Pd(110) is a thermally activated process and is accelerated at higher temperatures and oxygen pressures.²⁵ Recent temperature-programmed desorption measurements indeed confirm that a reduction in the sticking probability of oxygen parallels the formation of the subsurface oxygen.²⁶ Aside from influencing the oxygen sticking probability it is also feasible that any subsurface oxygen species reduces the adsorptive (binding) energy of CO on Pd(110); however, a direct confirmation on the basis of the presently available data material is not yet possible.

IV. DISCUSSION

In this discussion section we will start off with a brief summary of recently tackled problems and still open questions in the field of kinetic instabilities and oscillations as far as the CO oxidation over Pt and Pd single crystal surfaces is concerned, before we point to the beneficial role of phase-diagram studies in determining appropriate reaction mechanisms.

Mechanistic studies of oscillating reactions in heterogeneous catalysis such as oxidation of CO over platinum metal surfaces have mostly been concerned with the search for a mechanism that explains why there occur oscillations, and the system CO+O on the Pt(100) surface appears as one of the rare examples where this problem has been solved both experimentally⁴ and theoretically,²⁷ as we will briefly explain further below. From a more general point of view, the physical problem consists in finding one (or

more) surface related process(es) which, in addition to the simple Langmuir–Hinshelwood rate description given in Eqs. (1), can provide an enhancement or a modulation of the catalytic activity. This process takes the role of a feedback mechanism, and in order to function accordingly, it must be sufficiently slow. We emphasize again that the basic L-H reaction steps (viz., adsorption, desorption, and reaction) only lead to bistability, but do not predict any oscillatory behavior.²⁸

Constructing mechanisms and/or identifying feedback for oscillatory reactions becomes an enormous task when considering all of the possible processes involved (adsorption, desorption, diffusion, surface reaction, surface phase transition, e.g., reconstructions, subsurface species, and/or bulk compound formation, etc.). Even lateral adatom–adatom interactions (resulting in island formation or intimate mixing) may heavily influence the surface reactivity. Therefore, in our opinion the true mechanism can only be deduced rather indirectly from the conditions that influence the reaction. We refer again to the example of the Pt(100) surface. This surface can exist either in a (5×20) reconstructed or in a (1×1) unreconstructed form, whereby the (5×20) surface exhibits a low, the (1×1) configuration a high oxygen sticking probability. Furthermore, a critical CO coverage can transform the inherent (5×20) to a (1×1) phase. Taken together, by observing the two different surface structures during the oscillations and taking into account that an associated hysteresis in the CO adsorption–removal cycle provides the required time delay the oscillations could be understood in a straightforward manner.^{4,27} More difficult is the situation with the oscillations occurring during CO oxidation on Pt(110)²⁹ and Pt(210).^{7,8} Here the oscillatory behavior is more regular than with Pt(100) but can only be observed in a very narrow regime of external parameters. However, no significant change in the reactivity of these surfaces could be observed due to reconstruction or faceting of the surface, although attempts have been made to correlate the oscillations with faceting phenomena.^{30,31} Interestingly, the large hysteresis characteristic for the Pt(100) system does not occur on Pt(110) or Pt(210).^{5,28}

For higher pressure conditions (1 Torr < p_{O_2} < 760 Torr) on supported catalysts or polycrystalline samples, a model based on slow oxidation of the surface and recovery by reacting with CO has been suggested to explain the observed oscillations.^{6,32} In this case, too, the low reactivity of the surface for oxide formation could only be established indirectly. We note, however, that the slow formation and possible decomposition of a surface oxide can also play the part of a feedback process.

A much more direct experimental information that can help tracing the origin of oscillations are measurements and analyses of their amplitude and frequency—they are believed to display (at least to some extent) the time scale and coupling strength of the feedback process involved. However, a very high level of reproducibility of both frequencies and amplitudes still remains a challenging experimental requirement which is by no means easy to meet. The reason is that these two properties are sensitively af-

ected by a number of experimental parameters including, among many others, surface impurities and defects, reactor volume, sample size, flow rate, spatial self-organization, the process of synchronization of various surface domains, and nucleation processes of reactive surface waves. Our investigations of the Pt(210) system^{7,8} provided some clear examples here, where adsorption of impurities from the gas phase reactants caused a reduction in amplitude and frequency of the oscillation which sooner or later became extinguished. Furthermore, the formation of spatial reactive patterns consisting of CO and oxygen islands must in part be made responsible for the lack of oscillatory behavior in certain pressure and temperature regions. Obviously, the lack of strong coupling between various independently oscillating areas can cause irregular or even damped oscillations as observed with Pt(100), and on Pd(110) and Pt(110) aperiodic oscillations could be induced by changes in the coupling intensity through the gas phase.¹⁰

Another extremely valuable kind of information (which is much less affected by the aforementioned limitations) can nicely complement the mechanistic studies, namely, an experimental determination of the reactive phase diagram including the existence regions of the oscillations. In principle, these diagrams can provide the bifurcation points, the temperature dependence (role of desorption and diffusion) as well as the pressure dependence (role of adsorption) of the oscillations in question. Some experimental⁵ and theoretical examples³⁴ were previously reported for Pt(110) and (100) surfaces; however, the agreement between experiment and theoretical phase diagrams was not very satisfactory,³⁴ mainly due to limitations in the available experimental information on bifurcation diagrams. The lack of experimental observations in the existence region of oscillations for Pt surfaces is a consequence of the limited range of oxygen pressures accessible in the respective experiments. Our phase diagram for Pd(110) presented as Fig. 4 also exhibits a narrow oscillatory region for O₂ pressures below 10⁻² Torr. However, as the range of experimental parameters was extended, more features of the phase diagram became apparent. All in all, there are again a number of prerequisites for arriving at a reliable and complete phase diagram. These include the widest possible parameter variation, and a high degree of experimental reproducibility.

Not only do these requirements apply nicely to the Pd(110) system, but it is, in addition, the only system so far which exhibits untypical hysteresis diagrams near the oscillating region, cf., Fig. 3. What remains is the problem of explaining the observed cross-shaped phase diagram presented in Fig. 4. Boissonade and De Kepper³⁶ have demonstrated, based on a semiquantitative dynamical analysis, that the well-known Oregonator model of the BZ reaction³⁷ exhibits a characteristic cross-shaped phase diagram which expresses the relationship between bistability and oscillations in this system satisfactorily. Furthermore, additional insight gained by analyzing the oscillatory reaction and the control parameter, led Zhabotinskii *et al.*³⁸ to successfully replace the chemical feedback induced by the reaction by a direct electrochemical pumping feedback mechanism. This

demonstrates the validity of the analysis of oscillations in terms of bistability and feedback. Other chemical oscillating systems have exhibited similar phase diagrams²⁰ and have, due to their universal character, opened routes for finding new oscillatory systems and have even led to a successful design of new oscillators based on chlorite-ion chemistry.

Bassett and Imbihl have attempted to simulate the catalytic oscillations on Pd(110).³⁵ Their model resembles the oxide model first proposed in the group of Maple^{32,33} and assumes as feedback mechanism the formation of subsurface oxygen and its slow diffusion back to the surface. We have carried out a careful analysis of this model with the result that one obtains indeed a cross-shaped phase diagram; however it is inverted, i.e., oscillatory behavior is found for lower oxygen pressures and bistability for higher ones. This proves that coarse phase diagrams such as presented here, which simply locate regions of monostability, bistability, and oscillatory behavior in control parameter space, represent the minimal experimental information for a sensible analysis in terms of physical and chemical processes, since, in contrast with mathematical modeling, a description in terms of real system properties has to be *globally valid*. In a recent improved version of this model³⁹ it is assumed, among other things, that the activation barrier for the formation of subsurface oxygen depends on the oxygen coverage of the surface. An examination of this improved model revealed that, contrary to the opinion expressed in Ref. 35, this assumption is essential, because it yields a cross-shaped phase diagram with correct orientation. Though a step in the right direction, unfortunately this improved subsurface oxygen model does not reproduce the basic feature of the observed oscillatory behavior. Our simulations show that oscillations can only be induced when coming from the CO side, i.e., via the hard mode transition at τ_B , whereas it is found experimentally that the soft mode transition at τ_A occurs for both scan directions. Therefore, the subsurface oxygen model still needs improvement in order to explain at least the firmly established raw features of the phase diagram. It is the purpose of our presentation to provide accurate and reliable experimental material which can motivate other interested theoretical and experimental groups to investigate the fascinating phenomena occurring during the catalytic CO oxidation on Pd(110) surface.

ACKNOWLEDGMENT

The work was in part financed by the Deutsche Forschungsgemeinschaft through SFB 6.

¹ For a general description of the catalytic CO oxidation see, for example, T. Engel and G. Ertl, *Adv. Catal. Rel. Subj.* **28**, 1 (1979); T. Engel and G. Ertl, in *The Chemical Physics of Solid Surfaces and Heterogeneous Catalysis*, edited by D. A. King and D. P. Woodruff (Elsevier, Amsterdam, 1982), p. 73; G. Ertl, *Adv. Catal. Rel. Subj.* **37**, 213 (1990).

² For a recent review on oscillations see, for example: L. F. Razon and R. A. Schmitz, *Catal. Rev. Sci. Eng.* **28**, 89 (1986).

³ H. Beusch, P. Fieguth, and E. Wicke, *Adv. Chem. Ser.* **109**, 615 (1972); *Chem. Ing. Tech.* **44**, 445 (1972).

⁴ R. Imbihl, M. P. Cox, and G. Ertl, *J. Chem. Phys.* **84**, 3519 (1986).

- ⁵M. Eiswirth, P. Miller, K. Wetzl, R. Imbihl, and G. Ertl, *J. Chem. Phys.* **90**, 510 (1989).
- ⁶F. Schüth and E. Wicke, *Ber. Bunsenges. Phys. Chem.* **93**, 191 (1989).
- ⁷M. Ehsasi, M. Matloch, O. Frank, J. H. Block, K. Christmann, F. S. Rys, and W. Hirschwald, *J. Chem. Phys.* **91**, 4949 (1989).
- ⁸M. Ehsasi, S. Rezaie-Serej, J. H. Block, and K. Christmann, *J. Chem. Phys.* **92**, 7596 (1990).
- ⁹M. Ehsasi, C. Seidel, H. Ruppender, W. Drachsel, J. H. Block, and K. Christmann, *Surf. Sci.* **210**, L198 (1989).
- ¹⁰M. Ehsasi, O. Frank, J. H. Block, and K. Christmann, *Chem. Phys. Lett.* **165**, 115 (1990).
- ¹¹H. H. Rotermund, S. Jakubith, A. von Oertzen, and G. Ertl, *J. Chem. Phys.* **91**, 4942 (1989).
- ¹²H. H. Rotermund, W. Engel, M. Kordesch, and G. Ertl, *Nature* **343**, 355 (1990).
- ¹³M. Ehsasi, A. Karpowicz, M. Berdau, W. Engel, K. Christmann, and J. H. Block, *Ultramicroscopy* (in press).
- ¹⁴B. P. Belousov, *Sb. Ref. Radiat. Meditsin Za* (1958): (Collection of Abstracts on Radiation Medicine) 145 (Moskau, 1959).
- ¹⁵A. M. Zhabotinskii, *Biofizika* **2**, 306 (1964); *Oscillations in Biological and Chemical Systems* (Moskau, 1967).
- ¹⁶R. Reich, *Mathem. Naturw. Unterr.* **43**, 145 (1990).
- ¹⁷*Oscillations and Travelling Waves in Chemical Systems*, edited by R. J. Field and M. Burger (Wiley, New York, 1985).
- ¹⁸F. Schlögl, *Z. Phys.* **248**, 446 (1971); *ibid.* **253**, 147 (1972).
- ¹⁹F. Schlögl, *Ber. Bunsenges. Phys. Chem.* **84**, 351 (1980).
- ²⁰See Ref. 17, p. 223.
- ²¹V. I. Bykov, V. I. Elokhin, and G. S. Yablonskii, *React. Catal. Lett.* **4**, 191 (1976).
- ²²P. Fischer and U. M. Titulaer, *Surf. Sci.* **221**, 409 (1989).
- ²³S. Ladas, R. Imbihl, and G. Ertl, *Surf. Sci.* **219**, 88 (1989).
- ²⁴M. Wilf and P. T. Dawson, *Surf. Sci.* **65**, 399 (1977).
- ²⁵A. Hammoudeh, M. Ehsasi, K. Christmann, and J. H. Block (in preparation).
- ²⁶H. W. He and P. R. Norton, *Surf. Sci.* **204**, 26 (1988); *J. Chem. Phys.* **89**, 1170 (1988).
- ²⁷R. Imbihl, M. P. Cox, G. Ertl, H. Müller, and W. Brenig, *J. Chem. Phys.* **83**, 1578 (1985).
- ²⁸M. Ehsasi, Ph.D. thesis, Freie Universität Berlin, 1989.
- ²⁹M. Eiswirth and G. Ertl, *Surf. Sci.* **177**, 90 (1986).
- ³⁰S. Ladas, R. Imbihl, and G. Ertl, *Surf. Sci.* **197**, 153 (1988); *ibid.* **198**, 42 (1988).
- ³¹M. Sander, R. Imbihl, and G. Ertl, *J. Chem. Phys.* **95**, 6162 (1991).
- ³²J. E. Turner, B. C. Sales, and M. B. Maple, *Surf. Sci.* **193**, 54 (1981).
- ³³B. C. Sales, J. E. Turner, and M. B. Maple, *Surf. Sci.* **114**, 381 (1982).
- ³⁴Katharina Krischer, Ph.D. thesis, Freie Universität Berlin, 1990.
- ³⁵M. B. Bassett and R. Imbihl, *J. Chem. Phys.* **93**, 811 (1990).
- ³⁶J. Boissonade and P. De Kepper, *J. Chem. Phys.* **75**, 189 (1981).
- ³⁷P. De Kepper, I. R. Epstein, and K. Kustin, *J. Am. Chem. Soc.* **103**, 2133, 6621 (1981).
- ³⁸A. M. Zhabotinskii, A. N. Zaikin, and A. B. Rovinskii, *Kinet. Catal. Lett.* **20**, 29 (1982).
- ³⁹N. O. Hartmann, Master's thesis, Universität Bremen, 1992.